Apoptosis (2012) 17:916–925
DOI 10.1007/s10495-012-0737-y

ORIGINAL PAPER

Label-free monitoring of apoptosis by surface plasmon resonance detection of morphological changes

Jean-Sébastien Maltais · Jean-Bernard Denault · Louis Gendron · Michel Grandbois

Published online: 30 May 2012

Abstract Apoptosis can be routinely characterized using biomolecular markers such as in the TUNEL and the annexin V assays or by using fluorescent caspase substrates. Apoptosis can also be semi-quantitatively characterized using microscopy, which targets morphological features such as cell rounding, nuclear condensation and fragmentation as well as cell membrane blebbing. This label-free approach provides a limited resolution for the evolution of these events in time and relies heavily on subjective identification of the morphological features. Here we propose a label-free assay based on surface plasmon resonance (SPR) detection of minute morphology changes occurring as a result of apoptosis induction in an endothelial cell model (EA.hy926). At first, annexin V assays confirmed that our cellular model was responsive to TRAIL over a 12-hour period. Then, we show that SPR allows accurate monitoring of apoptosis by measuring (1) the duration of the latency period during which the apoptotic signal is integrated by the initiator caspases and transmitted to the executioner caspases, (2) the rate of the execution phase in which death substrates are cleaved and morphological changes occur, and (3) the total extent of apoptosis. Using these parameters, we characterized the responses obtained with TRAIL (EA.hy926, HeLa, AD-293) and the anti-Fas antibody (HeLa) for the extrinsic pathways and UV exposure (HeLa) for the intrinsic pathways. By comparing the SPR time-course of apoptosis with phase contrast micrographs, we demonstrate that the cell morphological hallmarks of apoptosis are the major contributors to the SPR signal. Altogether, our results validate the use of SPR as an accurate label-free assay for the real-time monitoring of apoptosis-triggered cell morphological changes.

Keywords Apoptosis assay · Surface plasmon resonance · Label-free · TRAIL · Cell morphology

Abbreviations

SPR	Surface plasmon resonance
RVU	Reflectance variation unit
HBSS	HEPES buffered salt solution
TRAIL	TNF (tumor necrosis factor)-related apoptosis-inducing ligand
PE	Phycoerythrin
7-AAD	7-aminoactinomycin D

Introduction

Apoptosis plays a pivotal role in various biological processes like morphogenesis [1] and immune system education and response [2]. The apoptotic cellular death can be triggered by several stimuli, including the binding of ligands to specific membrane receptors, DNA damage and growth factor starvation. Cell apoptosis involves a large variety of events for which a number of robust molecular markers exist. Among the most widely used are the TUNEL and annexin V assays [3–5] as well as various fluorogenic substrates for caspases [6, 7]. Semi-quantitative label-free assays also exist and usually involve the

J.-S. Maltais · J.-B. Denault · M. Grandbois (✉)
Département de Pharmacologie, Faculté de Médecine et des Sciences de la Santé, Université de Sherbrooke, 3001 12e Avenue Nord, Sherbrooke, QC J1H 5N4, Canada
e-mail: michel.grandbois@usherbrooke.ca

L. Gendron
Département de Physiologie et Biophysique, Faculté de Médecine et des Sciences de la Santé, Université de Sherbrooke, 3001 12e Avenue Nord, Sherbrooke, QC J1H 5N4, Canada

identification by microscopy of changes in morphological features occurring as the apoptotic process unravels (e.g., cell rounding, membrane blebbing as well as the condensation and fragmentation of the nucleus content [8, 9]). Although morphological assays are label-free, they normally provide only a limited time resolution for the evolution of apoptosis, as they rely on subjective identification of morphological features. As a result, there is a need for a cell-based and label-free technology that permits the quantification of morphological changes associated with the course of apoptosis.

The potential of such technologies has already been demonstrated for various cellular events using electric cell-substrate impedance sensing and optical biosensors using resonant waveguide gratings [10, 11]. Another promising candidate for label-free and cell-based assays is the surface plasmon resonance (SPR) biosensor. The resonance of a surface plasmon is a phenomenon occurring at the interface of a metal (often gold or silver) and a dielectric material when there is a match between the in-plane components of the wave vectors of the incident light and the surface plasmons. Consequently, an exponentially decaying evanescent field of approximately 200 nm is generated above the metal surface, which allows sensing of the refractive index change occurring within the evanescent field. The refractive index properties of the interface change when molecular redistribution occurs in the evanescent field, leading to a measurable shift in the angle at which maximum coupling (i.e. minimum reflectance) occurs. To date, SPR-based biosensing has been widely used in the biochemical characterization of molecular recognition processes in real-time and without labeling for a large variety of biological analytes on functionalized surfaces. This primary application of SPR has led to a large body of literature and is described in great details in several reviews [12–17]. However, proof of concept has been made that SPR biosensing can also be used in combination with living cells to monitor the effects of different molecular stimuli on cellular activities [18–21]. Notably, SPR has been used to study the ligand-induced reaction of mast cells [22], the activation of olfactory receptors by odorant molecules [23] and the stimulation of various cell receptors [24–26].

Here we applied SPR to the monitoring of apoptosis in living cells, taking advantage of the major cellular alterations and remodeling occurring in the course of the apoptotic reaction [27]. This allows us to study the relation that exists between the measured SPR signal and specific intracellular events leading to cell remodeling. Apoptosis can be induced via extrinsic pathways by the stimulation of the cell membrane death receptors 4-5 (DR4-5). These subunits multimerize and recruit the adaptor protein FADD to form a death-inducing signaling complex (DISC) [28]. This assembly promotes pro-caspase 8 activation by dimerization and self-cleavage, which induce cell death by activation of executioner caspases 3 and 7. Furthermore, in the so-called type II cells, the apoptotic signal requires the cleavage of Bid, which results in the activation of pro-caspase 9, which also leads to the activation of caspase 3 [29]. Following the activation of DR4-5, the cells enter a latent phase where there is no apparent sign of the death process [30]. This latency state is normally followed by the execution phase in which a sequence of apoptotic events lead ultimately to cell demise. Among the various consequences are considerable changes in cell morphology including rounding, nuclear condensation and fragmentation, membrane blebbing as well as cell detachment [31].

In this study, we used the SPR technique to monitor morphological changes produced by the activation of DR4-5 in endothelial cells. Cells were also monitored by phase contrast microscopy and conventional apoptosis assays using annexin V to determine the implication of cell apoptotic remodeling in the evolution of the SPR signal. We found that the SPR signal of apoptosis can be analyzed to quantify the duration of the latency period, the rate of the execution phase and the maximum extent of the apoptotic reaction. These parameters are used to establish a SPR signature of apoptosis, which is distinct from the responses produced by other molecules that also produce rounding, blebbing, detachment or disruption of the cellular membrane.

Materials and methods

SPR gold substrates

Microscope glass slides were cleaned in piranha solution and placed in a BOC Edwards Auto 306 evaporator for metal deposition under vacuum. A 3-nm adhesion layer of chromium and a 48-nm gold layer were deposited subsequently without breaking vacuum. SPR substrates were sterilized by autoclaving.

Cell culture

Human umbilical vein cells EA.hy926 (obtained from Dr. CJ Edgell, University of North Carolina, Chapel Hill, USA), AD-293 human embryonic kidney cells (Stratagene, La Jolla, CA, USA) and HeLa human cervical cancer cells (obtained from ATCC, Manassas, VA, USA) were maintained in Dulbecco's Modification Eagle's Medium (DMEM) supplemented with 10 % heat-inactivated fetal bovine serum (FBS), 2 mM L-glutamine, 2.5 μg/ml amphotericin B, 50 IU/ml penicillin and 50 μg/ml streptomycin (Wisent, St-Bruno, QC, Canada) at 37 °C in a 5 %

CO_2 incubator. 30 μg/ml endothelial cell growth supplements (BD Biosciences, Bedford, MA, USA) were added to EA.hy926 cells in order to preserve phenotype. EA.hy926 and HeLa cells were cultured directly on SPR substrates whereas the gold substrates for AD-293 cells were coated with poly-L-lysine (Sigma, Oakville, ON, Canada) to promote adhesion. TRAIL was acquired from Enzo Life Sciences (Plymouth Meeting, PA, USA), anti-Fas mAb from Kamiya Biomedical (Seattle, WA, USA), Z-VAD-FMK from R&D Systems (Minneapolis, MN, USA), sodium azide from Sigma-Aldrich (Oakville, ON, Canada), trypsin from Wisent (St-Bruno, QC, Canada) and SDS from Invitrogen (Carlsbad, CA, USA).

SPR analysis

The SPR measurements were performed at 37 °C in a pH 7.4 HEPES-Buffered Salt Solution (HBSS), composed of 20 mM HEPES, 120 mM NaCl, 5.3 mM KCl, 1.8 mM $CaCl_2$, 0.8 mM $MgSO_4$, 11.1 mM dextrose, 50 IU/ml penicillin and 50 μg/ml streptomycin. The custom-built SPR apparatus was equipped with a 4 mW stabilized laser diode with a wavelength of 635 nm (Thorlabs, Inc., USA). As illustrated in Fig. 1a, the beam is refracted through a BK7 coupling prism ($n = 1.515$; Melles Griot, USA) and a layer of matching refractive index fluid (Cargille Laboratories, NJ, USA) before being reflected off the gold surface and passed through a polarizing beamsplitter sending p-polarization and s-polarization into two different photodetectors. Unlike p-polarization, s-polarization is unaffected by surface plasmons, allowing its use as a control to remove time-dependent noises such as laser power drift and temperature variations. Before each experiment, an angular scan was performed, in which the laser beam is reflected on the gold surface at different incident angles to identify the quasi-linear portion of the curve. In Fig. 1b, we show an example of angular scans where the curves shift to the left over time indicating a decrease in the refractive index in the evanescent field. However, to monitor the shifts of the angular scan in real-time, measurements were taken at a fixed angle of approximately 71°. In this case, the SPR signal is represented as an increase or a decrease in the measured reflectance at this fixed angle for the duration of the experiment (Fig. 1c). Results were analyzed in a custom-developed LabVIEW program and plotted in reflectance variation units (RVU) where 1 RVU represents a 0.1 % variation in total reflectance.

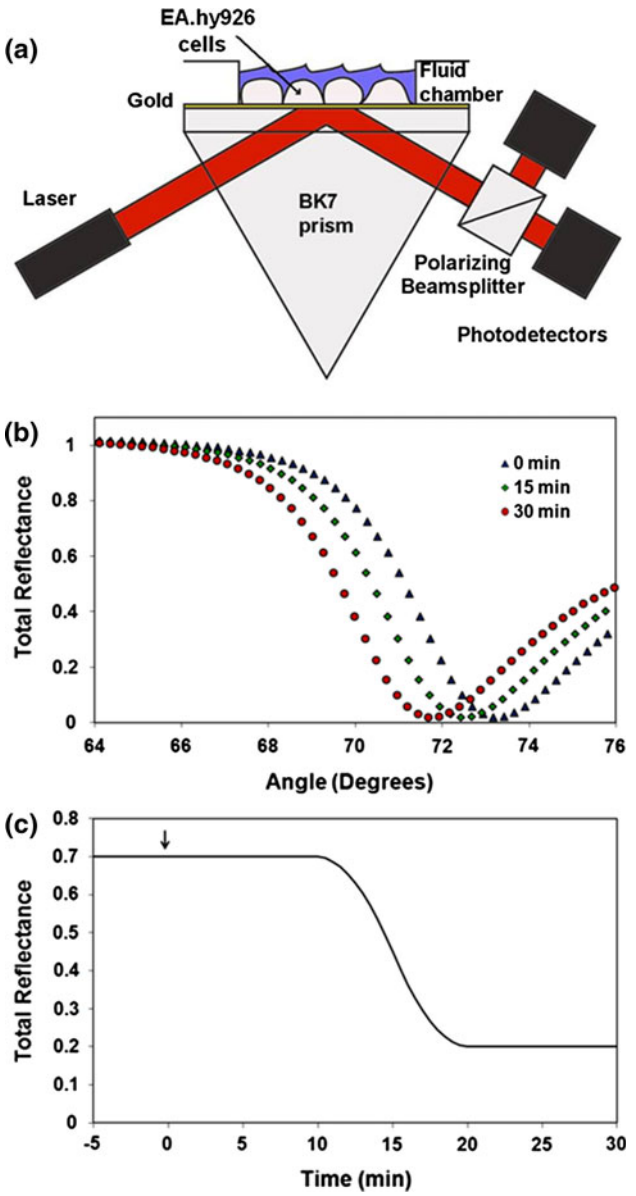

Fig. 1 **a** Schematic representation of the SPR apparatus. A 635 nm laser diode is reflected on a gold-coated glass slide, over which a cell layer is grown to confluence. The intensity of the reflected laser beam is measured by 2 photodetectors after being divided by a polarizing beamsplitter. S-polarization of the laser beam is used as a reference to remove time-dependent noises since it is unaffected by surface plasmons. **b** Example of angular scans in which the intensity of the reflected laser beam varies depending on the incident angle with the gold surface. *Curves* shifting to the left are typically due to a decrease in the refractive index in the sensing area. **c** Example of an experiment performed at a fixed incident angle of approximately 71°. A decrease in the measured reflectance is typically due to a diminution in the refractive index in the sensing area

Phase contrast microscopy

Morphological changes were observed by phase contrast microscopy. EA.hy926 cells grown on SPR substrates were placed in HBSS medium at 37 °C before stimulation. Micrographs were acquired with a fluorescence inverted microscope (AxioVert 200, Carl Zeiss, Germany) equipped with a phase contrast system with a 20× objective, a high

sensitivity camera (AxioCam MRm, Carl Zeiss, Germany) and analyzed using AxioVision LE software. The sequence of micrographs in Fig. 4b–g was recorded with an inverted fluorescence microscope (AE31, Motic) equipped with a phase contrast system in combination with a 20× objective and a PixelFly QE camera (PCO, Germany) and analyzed using CamWare 3.05.

Annexin V assays

EA.hy926 cells were stimulated with TRAIL in HBSS (same conditions as for SPR assays) at 37 °C and were recovered using trypsin. Cells were suspended at a concentration of 2×10^5 cells/ml and a equivalent volume of Guava Nexin Reagent (Guava Technologies, Hayward, CA, USA) was added. Samples were let to incubate 20 min at room temperature in the dark before measuring fluorescence of annexin-PE and 7-AAD by flow cytometry (Guava EasyCyte Mini, Millipore, USA). Data were analyzed with the provided Guava Cytosoft Software.

Statistics

Data presented in Table 1 are shown as mean value ± standard error of the mean (SEM).

Results and discussion

Annexin V assays on EA.hy926 cells

To demonstrate that SPR can be used as a label-free approach for real-time monitoring of apoptosis, we used the immortalized endothelial cell line EA.hy926. To confirm that these cells are sensitive to the apoptotic inducer TRAIL, we performed annexin V binding assays in which the early caspase activation leads to the externalization of membrane phosphatidylserines. The cell viability stain 7-aminoactinomycin D (7-AAD) was used concurrently to assess the integrity of the cell membrane. Labeled cells were collected and analyzed by flow cytometry at different time points after TRAIL exposure. The dot plots in Fig. 2 show data for both annexin V-PE and 7-AAD. In Fig. 2a, the cells were immediately collected after stimulation with 10 ng/ml TRAIL. In these conditions, the cells were found mainly in the bottom-left corner of the dot plot, which confirms that most cells are intact and viable. The dot plot in Fig. 2b was obtained after 12 h of TRAIL stimulation and shows distinct populations of cells in both the early (bottom-right) and late (upper-right) apoptotic states. The evolution of living cells (annexin V-PE and 7-AAD negative) as a function of time is presented in Fig. 2c. Notably, the annexin V assay, which is known to be sensitive to

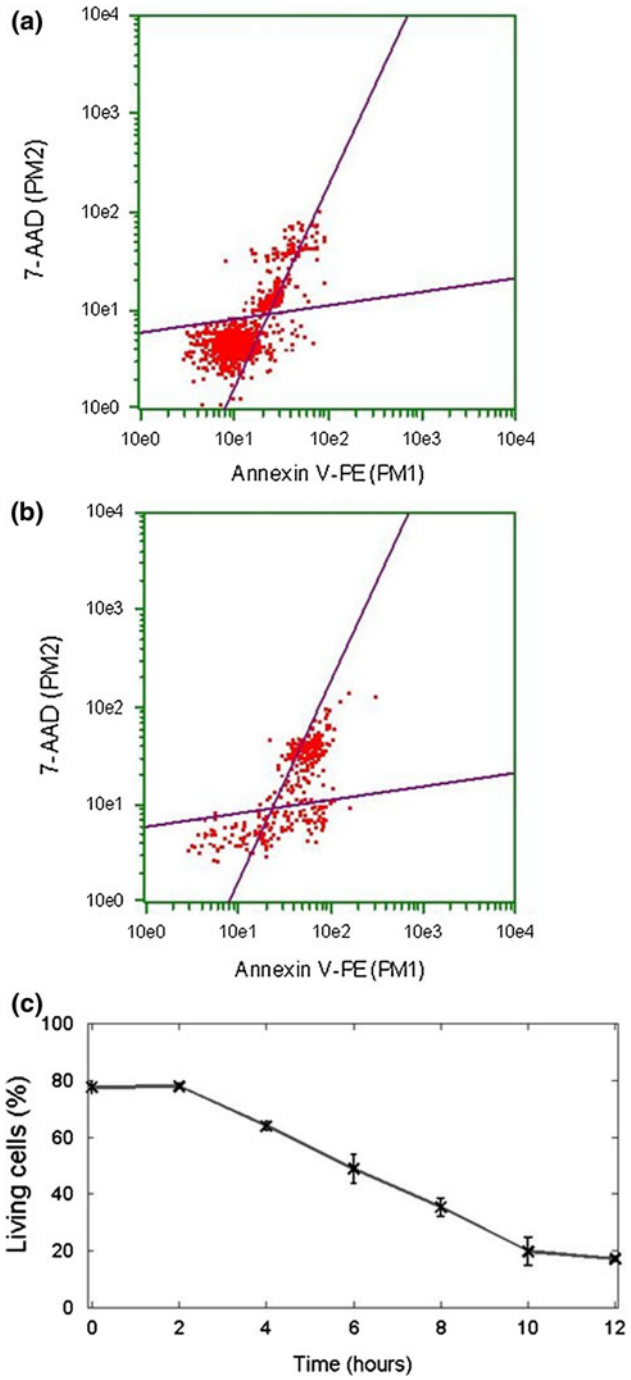

Fig. 2 Typical FACS analysis *dot plots* showing the evolution of EA.hy926 cells apoptosis after **a** 0 h and **b** 12 h of treatment with 10 ng/ml TRAIL. Annexin V-PE detects apoptosis by binding to externalized phosphatidylserines and 7-AAD is used as a cell viability marker. Quadrants have been assigned according to Guava Technologies' protocol **c** Survival curve (i.e. annexin V and 7-AAD negative) of EA.hy926 cells treated with 10 ng/ml TRAIL over a 12 h time-course. In these experimental conditions and using this analytical method, ~22 % of control cells display apoptotic features. The data are averaged ± SEM from 4 independent experiments. PM1 and PM2 correspond to the two detection channels

early apoptotic events, did not detect any fluorescence change in the first 2 h of stimulation, after which the number of living cells gradually decreased to <18 % after 12 h. These results confirm that EA.hy926 are sensitive to a nominal dose of TRAIL, and thus can be used to validate SPR-based apoptosis assays.

SPR angular scan of a cell monolayer

SPR measures the molecular density at the interface of a gold surface and the basal region of a cell monolayer. To confirm that SPR can detect the cellular mass redistribution associated with apoptotic events, we cultured EA.hy926 cells to confluence on gold substrates. In a typical experiment, an angular scan (Fig. 3a) was initially performed to identify the angle at which maximum resonance between the laser beam and the gold surface plasmons occurs. This condition, which corresponds to a minimum in the intensity of the reflected laser beam, occurred at 73,5° on the angular scan obtained before TRAIL stimulation. After 12 h of stimulation with 10 ng/ml of TRAIL, the entire angular scan shifts to the left and the optimal coupling occurs at 72°. A shift of the angular scan to the left is associated with a diminution of the molecular density in the evanescent field, such as in hypo-osmolar conditions producing a dilution of the cytoplasmic components [21] or in cell contraction creating intercellular gaps [24]. The shift of the angular scan after TRAIL stimulation is consistent

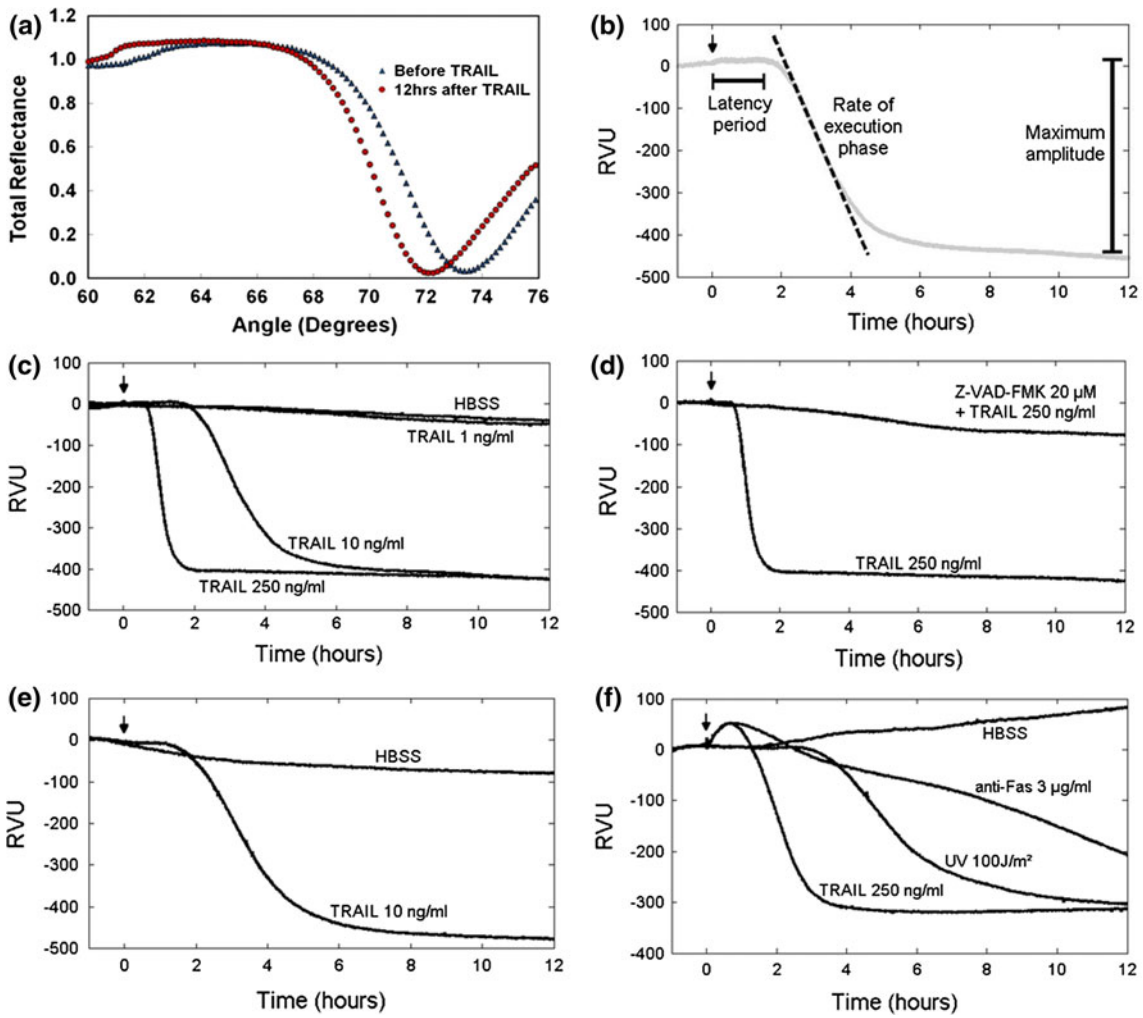

Fig. 3 **a** Angular scans taken on SPR substrates covered with a EA.hy926 cell monolayer in HBSS before (*blue triangles*) and after (*red circles*) a 12 h treatment with 10 ng/ml TRAIL. **b** Parameters extracted from the apoptosis SPR signature. **c** Reflectance measurements over a 12 h period after stimulation with increasing concentrations of TRAIL. **d** Reflectance measurements of cells exposed to 250 ng/ml TRAIL with or without a 1 h pretreatment with 20 µM caspase inhibitor Z-VAD-FMK. **e** Reflectance measurements of AD-293 cells treated with 10 ng/ml TRAIL or HBSS only over a 12 h period. **f** Reflectance measurement of HeLa cells treated with HBSS only, 250 ng/ml TRAIL, 3 µg/ml anti-Fas mAb or 100 J/m^2 UV. The moment of the stimulation is marked by an arrow. Data is expressed in reflectance variation units (RVU) where 1 RVU represents 0.1 % in total reflectance. All experiments were reproduced at least four times (Color figure online)

with apoptotic events such as cell rounding, membrane blebbing and cell detachment from the surface, which are assumed to cause an important change in molecular density at the gold-sensing surface.

SPR monitoring of apoptosis

Apoptosis involves a complex temporal sequence of molecular and morphological events defining the so-called induction and execution phases ultimately culminating in the cell death. In order to monitor the apoptotic process in real-time, the SPR signal was recorded at a fixed angle selected from the linear portion of the curve between 70° and 73° and expressed as reflectance variation units (RVU) as a function of time. Hence, translations of the angular scan can be monitored in real-time following various treatments; a shift to the left representing a loss in the reflectance signal and inversely. As shown in Fig. 3b, before stimulation, the measured reflectance is stable and is indicative of a steady level of cellular activity. After addition of 10 ng/ml of TRAIL, we observed an important decrease in reflectance, consistent with the time-course observed in the annexin V assay. The SPR signal comes from a few thousand cells from a sensing area of 0.5 mm^2. Hence, it represents a convolution of the responses of all individual cells. Therefore, the measured latent phase corresponds to the time at which significant change occurs in the cell population as a result of initiation of apoptosis. Similarly, the maximum rate occurs when a maximum number of cells undergo apoptosis. Three parameters can be extracted from the SPR signal signature to reflect the evolution of the apoptosis reaction: (1) the length of the latency period which corresponds to the time between the TRAIL addition and the onset of the SPR signal change, (2) the rate of the execution phase, which is the maximum slope measured after the stimulation and (3) the global extent of the apoptotic reaction which corresponds to the difference between the initial and final plateaus. As expected, these parameters were found to vary following cell treatment with increasing doses of TRAIL (Fig. 3c; Table 1). One ng/ml TRAIL is inefficient to initiate apoptosis in EA.hy926 cells and compares with cells subjected to HBSS only (control) with a SPR signal varying over a few tens of RVU. For these conditions, the rate of the execution phase as well as the duration of the latency period were not significant or could not be determined. In contrast, at the higher TRAIL doses of 10 and 250 ng/ml, one can observe a clear effect of TRAIL on all three SPR signal parameters. Firstly, the duration of the latency period was 75.9 ± 5.3 min and 37.8 ± 5.1 min, respectively. Additionally, the rate of the execution phase increased to 3.1 ± 0.6 and 13.2 ± 1.2 RVU/min and the maximum amplitude of the SPR signal variation also increased to 431.9 ± 48.8 and 459.9 ± 56.3 RVU, respectively. The rate of the execution phase could also be expressed as % of apoptosis/min (% Apo/min) by assuming a 100 % apoptotic cell population for the maximum amplitude of the SPR signal observed at 250 ng/ml. This gives a rate equal to 0.68 ± 0.13 and 2.87 ± 0.27 %Apo./min at 10 and 250 ng/ml, respectively. Not surprisingly, these results suggest that after a TRAIL concentration threshold is reached, the maximum extent of apoptosis will be observed and that the TRAIL dose level will mainly affect the duration of the latency period and the rate at which the execution phase proceeds. The SPR experiment with the pan-caspase inhibitor Z-VAD-FMK (20 μM) confirms this interpretation of the SPR signal signature since it prevented the onset of the apoptotic reaction even at the highest concentration of TRAIL (Fig. 3d). Additional SPR experiments have been performed with AD-293 cells, a derivative of the commonly used HEK293 cell line with improved cell adherence, that are sensitive to TRAIL-induced apoptosis [32]. AD-293 cells treated with 10 ng/ml of TRAIL exhibit a SPR pattern and parameters that are similar to EA.hy926 cells treated with the same conditions (Fig. 3e). To further demonstrate its applicability in the context of apoptosis, we performed additional experiments with HeLa cells, which are sensitive to various inducers of apoptosis. Extrinsic pathways were activated with either TRAIL (250 ng/ml) or anti-Fas antibodies (3 μg/ml; Fig. 3f). While both agents induce apoptosis, they present distinct response kinetics. As TRAIL-treated cells responded similarly, anti-Fas-treated cells produced a steady decrease in the refractive index over time, showing only partial apoptosis after 12 h. Interestingly, the latency phases of EA.hy926 and HeLa cells are different which indicate a distinct sensitivity to the stimulus. In addition, a slight increase can be observed in the measured reflectance

Table 1 SPR data on parameters extracted from the apoptosis signatures obtained with EA.hy926 cells

	Length of latency period (min)	Rate of execution phase (RVU/min)	Maximum amplitude (RVU)
HBSS	–	–	36.7 ± 13.4
TRAIL 1 ng/ml	–	–	48.4 ± 16.4
TRAIL 10 ng/ml	75.9 ± 5.3	3.14 ± 0.59	431.9 ± 48.8
TRAIL 250 ng/ml	37.8 ± 5.1	13.20 ± 1.23	459.9 ± 56.3
Z-VAD-FMK 20 μM + TRAIL 250 ng/ml	–	–	44.1 ± 29.2

in the minutes following stimulation of apoptotic extrinsic pathways. This feature which is likely due to a subtle spreading of the cell body could be used to delineate the molecular mechanisms associated with the early phase of apoptosis in specific cell types. The intrinsic pathways were activated using an UV exposure of 100 J/m^2. In these cells, apoptosis was observed in a TRAIL-like pattern but with a considerably longer latent period. This lag time could be associated to the initiation phase in which signal is integrated by the initiator caspases and transmitted to the executioner caspases until a threshold is reached after which death substrates are cleaved and morphological changes occur. Once the apoptosis SPR signature for a given cell model exposed to a given concentration of a specific apoptosis inducer is known in terms of the duration of the latency phase and maximum rate, it should be possible to identify the impact of any additional modulation of the molecular apoptotic pathway simply by quantifying variations from the original SPR signal. Altogether, these results suggest that SPR monitoring of apoptosis is applicable to a wide range of adhering cell lines and apoptotic inducers.

Attribution of the SPR signal in relation to cell morphology

Executioner caspases are necessary for several apoptosis-related morphological changes. Particularly, caspases 3 and 6 cleave lamins which are responsible of maintaining the structural activity of the nucleus [33]. Caspases promote the formation of blebs and cell rounding by the reorganization of actin into a ring-like structure [34, 35]. In addition, early detachment of cells from the extracellular matrix is caused by caspase-dependent cleavage of focal adhesion proteins [36] and microtubule disassembly [37]. A dying cell could even signal to neighboring cells for its extrusion from the cell layer through an actin-myosin-dependent mechanism [38]. In order to establish a relation between those morphological changes and the SPR signal, we compared a time sequence of phase contrast micrographs obtained following the addition of 10 ng/ml of TRAIL, with its corresponding SPR profile (Fig. 4). The phase contrast micrographs were selected at different times at specific regions on the SPR curve (Fig. 4a). At $t = 0$ min (Fig. 4b), the cell monolayer was intact with few cells adopting a round shape commonly attributed to apoptotic cells. In micrographs taken during the latency period (Fig. 4c, d), no significant morphology changes are observed, which is consistent with the SPR signal. In contrast, after the initial latency period, an increasing population of round cells is visible and they progressively detach from the surface (Fig. 4e–i) as a function of time. Since the evanescent field senses mass redistribution in a

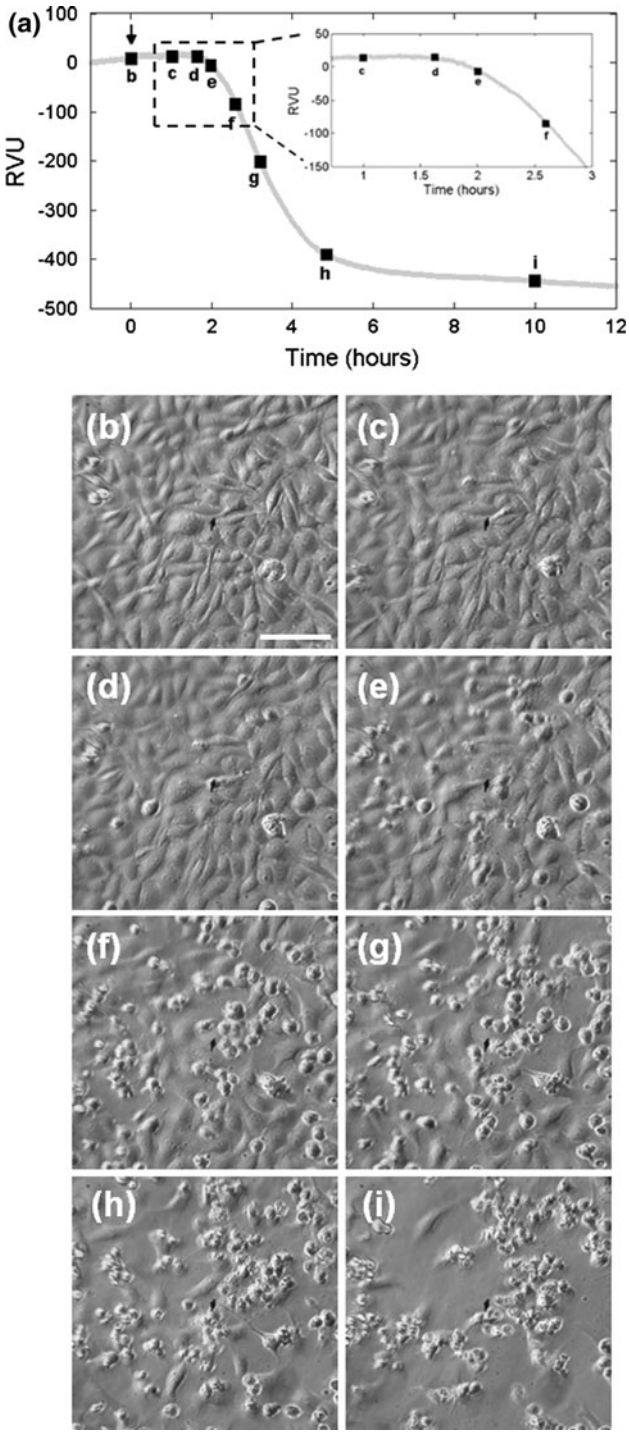

Fig. 4 Correlation between the apoptosis SPR signal and cell morphology. **a** Selected time points on the SPR signature at which micrographs were taken after EA.hy926 cells stimulation with 10 ng/ml TRAIL. **b–i** Phase contrast micrographs taken at corresponding times showing the evolution of apoptosis-related morphological changes over 12 h. The *scale bar* represents 200 μm

200 nm region above the gold surface, morphological events caused by apoptosis, such as cell rounding, nuclear fragmentation, cleavage of adhesion proteins causing cell

detachment and rupture of the cellular membrane, could be easily detected by SPR. Overall, these observations suggest that variation in cell morphology represents a major contribution to the SPR signal which can be potentially addressed through time-resolved SPR measurement.

The sensing area including several thousand cells provides strong statistics on the cell population behavior. Despite the large number of cells monitored, these results give an insight into the high sensitivity of SPR and its ability to monitor subtle changes in cell morphology. As observed in Fig. 4d and e, only a few cells undergoing apoptosis are enough to produce a measurable reflectance decrease. From this perspective, the use of SPR with microscopy brings quantitative measurements to the subjective observations obtained with microscopy alone. One can accurately extract temporal parameters such as the latency period before the onset of major cell morphological changes. As seen in the sequence of phase contrast micrographs, this parameter cannot be unambiguously determined from comparison of Fig. 4c–e. Additionally, the rate at which the active phase of apoptosis occurs can be quantified as the maximum slope measured in Fig. 4a. This parameter is not easily quantified from either a sequence of micrograph or by running movies of the apoptotic reaction. SPR also offers a significant advantage over traditional apoptosis methods, such as TUNEL and annexin V assays, in that SPR always monitors the same cell population throughout the whole experiment. This particularity allows the early detection of apoptosis in an accurate and time-resolved manner without the variations associated to different cell populations and experiments done at fixed time intervals. By offering better time-resolution of the apoptotic reaction, SPR represents a valuable alternative to study events like the initiation of apoptosis and the speed of the response once the process is triggered.

Given the sensitivity of SPR measurement for cell morphological changes and to confirm that the SPR signature identified is unique to apoptosis, we compared SPR signatures obtained for biological agents well known to induce cell shrinking, cleavage of adhesion proteins or break of the cellular membrane in living cells. Firstly, 2 % SDS was used to induce an immediate rupture and dissolution of the cellular membrane, the nuclear membrane and the release of intracellular matrix. In contrast to what is observed following TRAIL treatment, the SPR curve (Fig. 5a) recorded following SDS treatment shows an immediate loss in reflectance due to cells quickly disappearing from the surface (Fig. 5b) in <30 s, as opposed to TRAIL-treated cells which showed a latent phase of more than 75 min following the stimulation. Moreover, the SPR signal of SDS-treated cells reaches a plateau in <30 s while the signal of TRAIL-treated cells takes hours to reach a plateau. This result is indicative of the maximum amplitude in the SPR signal that can be attained as a result of cells completely eliminated from the sensing surface. Trypsin at a concentration of 0.2 % was used to induce cell detachment by cleaving the cell protein attachments to the surface. As seen in the SPR signal, the onset of the process was found to be very rapid and reached completion in <10 min. However, the maximum reflectance loss was presumably limited by the fact that cells stay in proximity to the sensing surface even after the action of the enzyme. Interestingly, a slow but steady reflectance increase can be observed over time and could be due to weakening trypsin activity and cells gradually reattaching onto the substrate. Finally, at a concentration of 5 mg/ml, sodium azide (NaN_3), a toxin preventing cellular respiration, produced a notable decrease in the measured reflectance in the first 5 min (Fig. 5a), which correlates with the shrinking of the cells shown in Fig. 5b. At this concentration, the SPR signal was found to stabilize after some time, a feature that could be attributed to the reversible character of this cell

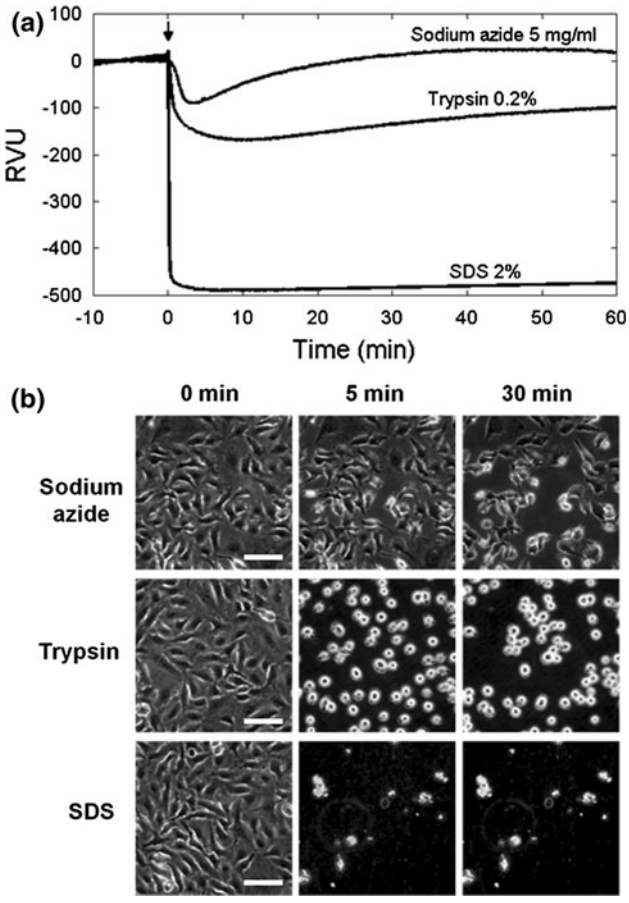

Fig. 5 **a** Reflectance measurements of EA.hy926 cells treated with 5 mg/ml sodium azide, 0.2 % trypsin or 2 % SDS over 1 h. The curves are typical from sets of three experiments for each condition **b** Phase contrast micrographs taken before, 5 min after and 30 min after stimulation with sodium azide, trypsin or SDS. *Scale bars* represent 100 μm

perturbation for a portion of the cell population. It should also be mentioned that the SPR signature for TRAIL-induced apoptosis is distinct from the one produced when G-protein coupled receptors such as the angiotensin and thrombin receptors are stimulated [24, 25]. Altogether, these results suggest that cell rounding, detachment from substrate or loss of cellular membrane integrity can be easily monitored by SPR and that these events contribute to the SPR signature associated with cell apoptotic events. Indeed, the SPR signature of apoptosis is likely to be caused by a unique combination of molecular and morphological events occurring in the execution phase of apoptosis.

Conclusion

In the present study, we have described a novel assay based on SPR monitoring of cellular events associated with apoptosis in living cells. SPR is a label-free technique that can detect a large range of events simultaneously on the same cell population. As a real-time assay, it provides time-resolved details of global cellular changes occurring as a result of apoptosis. Cell rounding, membrane blebbing, nuclear fragmentation and cell detachment are all events that are highly ubiquitous, making SPR a relevant method to monitor the global progress of the apoptosis reaction for a wide range of cells and apoptosis inducers. Flow cytometry experiments performed with two molecular markers for apoptosis confirmed that the endothelial cell model EA.hy926 responded to TRAIL, a robust inducer of apoptosis. The monitoring of the SPR signal as a function of time for a cell monolayer treated with TRAIL allowed the quantification of three parameters of the apoptotic reaction. Firstly, we measured the duration of the latency period in which the signal is integrated by the initiator caspases and transmitted to the executioner caspases until a threshold is reached leading to death substrates cleavage and cell morphological changes. The SPR signal signature also allowed extraction of the rate at which these changes occur as well as the maximum amplitude of the apoptotic reaction. Comparison with a time sequence of phase contrast images obtained following TRAIL stimulation, SDS exposure, trypsin and sodium azide treatments confirmed that morphological changes in cells were the major contribution to the SPR signal. Although it will not replace conventional label-based assays for apoptosis in terms of sensitivity and selectivity, the SPR assay represents a simple label-free approach to potentially address the mechanisms associated with the latency periods as well as the rate at which apoptosis occurs. The analysis of these parameters could provide a simple tool for the screening of compounds interfering with apoptosis at various levels.

Acknowledgments The authors would like to acknowledge Yannick Miron for his technical help with the SPR apparatus and Véronique Blais for her support with flow cytometry analyses. This research was supported by funds from the Canadian Institutes of Health Research (CIHR) and the Natural Sciences and Engineering Research Council of Canada (NSERC) to MG, LG and JBD.

Conflict of interest The authors declare no conflict of interests.

References

1. Kuranaga E, Matsunuma T, Kanuka H, Takemoto K, Koto A, Kimura K, Miura M (2011) Apoptosis controls the speed of looping morphogenesis in drosophila male terminalia. Development 138(8):1493–1499
2. Feig C, Peter ME (2007) How apoptosis got the immune system in shape. Eur J Immunol 37(Suppl 1):S61–S70
3. O'Brien IE, Reutelingsperger CP, Holdaway KM (1997) Annexin-V and TUNEL use in monitoring the progression of apoptosis in plants. Cytometry 29(1):28–33
4. van Engeland M, Nieland LJ, Ramaekers FC, Schutte B, Reutelingsperger CP (1998) Annexin V-affinity assay: a review on an apoptosis detection system based on phosphatidylserine exposure. Cytometry 31(1):1–9
5. Heatwole VM (1999) TUNEL assay for apoptotic cells. Methods Mol Biol 115:141–148
6. Cen H, Mao F, Aronchik I, Fuentes RJ, Firestone GL (2008) DEVD-NucView488: a novel class of enzyme substrates for real-time detection of caspase-3 activity in live cells. FASEB J 22(7):2243–2252
7. Zhang HZ, Kasibhatla S, Guastella J, Tseng B, Drewe J, Cai SX (2003) N-Ac-DEVD-N′-(Polyfluorobenzoyl)-R110: novel cell-permeable fluorogenic caspase substrates for the detection of caspase activity and apoptosis. Bioconj Chem 14(2):458–463.
8. Coleman ML, Sahai ES, Yeo M, Bosch M, Dewar A, Olson MF (2001) Membrane blebbing during apoptosis results from caspase-mediated activation of ROCK I. Nat Cell Biol 3(4):339–345.
9. Ziegler U, Groscurth P (2004) Morphological features of cell death. News Physiol Sci 19:124–128
10. Fang Y, Li G, Ferrie AM (2007) Non-invasive optical biosensor for assaying endogenous G protein-coupled receptors in adherent cells. J Pharmacol Toxicol Methods 55(3):314–322
11. Scott CW, Peters MF (2010) Label-free whole-cell assays: expanding the scope of GPCR screening. Drug Discov Today 15(17–18): 704–716
12. Boozer C, Kim G, Cong S, Guan H, Londergan T (2006) Looking towards label-free biomolecular interaction analysis in a high-throughput format: a review of new surface plasmon resonance technologies. Curr Opin Biotechnol 17(4):400–405
13. McDonnell JM (2001) Surface plasmon resonance: towards an understanding of the mechanisms of biological molecular recognition. Curr Opin Chem Biol 5(5):572–577
14. Pattnaik P (2005) Surface plasmon resonance: applications in understanding receptor–ligand interaction. Appl Biochem Biotechnol 126(2):79–92
15. Jason-Moller L, Murphy M, Bruno J (2006) Overview of biacore systems and their applications. Curr Protoc Protein Sci; Chapter 19:Unit 19.13
16. Danielson UH (2009) Fragment library screening and lead characterization using SPR biosensors. Curr Top Med Chem 9(18): 1725–1735
17. de Mol NJ (2012) Surface plasmon resonance for proteomics. Methods Mol Biol 800:33–53.

18. Hide M, Tsutsui T, Sato H, Nishimura T, Morimoto K, Yamamoto S, Yoshizato K (2002) Real-time analysis of ligand-induced cell surface and intracellular reactions of living mast cells using a surface plasmon resonance-based biosensor. Anal Biochem 302(1):28–37.
19. Yanase Y, Suzuki H, Tsutsui T, Hiragun T, Kameyoshi Y, Hide M (2007) The SPR signal in living cells reflects changes other than the area of adhesion and the formation of cell constructions. Biosens Bioelectron 22(6):1081–1086
20. Suzuki H, Yanase Y, Tsutsui T, Ishii K, Hiragun T, Hide M (2008) Applying surface plasmon resonance to monitor the IgE-mediated activation of human basophils. Allergol Int 57(4): 347–358
21. Robelek R, Wegener J (2010) Label-free and time-resolved measurements of cell volume changes by surface plasmon resonance (SPR) spectroscopy. Biosens Bioelectron 25(5):1221–1224
22. Tanaka M, Hiragun T, Tsutsui T, Yanase Y, Suzuki H, Hide M (2008) Surface plasmon resonance biosensor detects the downstream events of active PKCbeta in antigen-stimulated mast cells. Biosens Bioelectron 23(11):1652–1658
23. Lee SH, Ko HJ, Park TH (2009) Real-time monitoring of odorant-induced cellular reactions using surface plasmon resonance. Biosens Bioelectron 25(1):55–60
24. Cuerrier CM, Chabot V, Vigneux S, Aimez V, Escher E, Gobeil F, Charette PG, Grandbois M (2008) Surface plasmon resonance monitoring of cell monolayer integrity: implication of signaling pathways involved in actin-driven morphological remodeling. Cell Mol Bioeng 1(4):229–239.
25. Chabot V, Cuerrier CM, Escher E, Aimez V, Grandbois M, Charette PG (2009) Biosensing based on surface plasmon resonance and living cells. Biosens Bioelectron 24(6):1667–1673
26. Homola J (2003) Present and future of surface plasmon resonance biosensors. Anal Bioanal Chem 377(3):528–539.
27. Al-Rubeai M, Fussenegger M (eds) (2004) Cell engineering: apoptosis. Kluwer, Dordrecht
28. Sheridan JP, Marsters SA, Pitti RM, Gurney A, Skubatch M, Baldwin D, Ramakrishnan L, Gray CL, Baker K, Wood WI, Goddard AD, Godowski P, Ashkenazi A (1997) Control of TRAIL-induced apoptosis by a family of signaling and decoy receptors. Science 277(5327):818–821
29. Wang S, El-Deiry WS (2003) TRAIL and apoptosis induction by TNF-family death receptors. Oncogene 22(53):8628–8633.
30. Kaufmann SH (ed) (1997) Apoptosis: pharmacological implications and therapeutic opportunities. Academic Press, San Diego
31. Melino G, Vaux D (eds) (2010) Cell Death. Wiley–Blackwell, Oxford
32. Boucher D, Blais V, Drag M, Denault JB (2011) Molecular determinants involved in activation of caspase 7. Biosci Rep 31(4):283–294
33. Rao L, Perez D, White E (1996) Lamin proteolysis facilitates nuclear events during apoptosis. J Cell Biol 135(6 Pt 1): 1441–1455
34. Mashima T, Naito M, Noguchi K, Miller DK, Nicholson DW, Tsuruo T (1997) Actin cleavage by CPP-32/apopain during the development of apoptosis. Oncogene 14(9):1007–1012.
35. Hacker G (2000) The morphology of apoptosis. Cell Tissue Res 301(1):5–17
36. Wen LP, Fahrni JA, Troie S, Guan JL, Orth K, Rosen GD (1997) Cleavage of focal adhesion kinase by caspases during apoptosis. J Biol Chem 272(41):26056–26061
37. Mills JC, Lee VM, Pittman RN (1998) Activation of a PP2A-like phosphatase and dephosphorylation of tau protein characterize onset of the execution phase of apoptosis. J Cell Sci 111(Pt 5):625–636
38. Rosenblatt J, Raff MC, Cramer LP (2001) An epithelial cell destined for apoptosis signals its neighbors to extrude it by an actin- and myosin-dependent mechanism. Curr Biol 11(23): 1847–1857